

1 **Impairments in *SHMT2* expression or cellular folate availability reduce oxidative**
2 **phosphorylation and pyruvate kinase activity**

3 Authors: Joanna L. Fiddler¹, Jamie E. Blum^{1,2}, Luisa F. Castillo¹, Anna E. Thalacker-Mercer³
4 and Martha S. Field¹

5 Author affiliations:

6 ¹Division of Nutritional Sciences, Cornell University, Ithaca, New York USA

7 ²Department of Chemical Engineering, Stanford University, Stanford, California USA

8 ³Department of Cell, Developmental and Integrative Biology, University of Alabama at
9 Birmingham, Birmingham, Alabama USA.

10

11 To whom correspondence should be addressed: Martha S. Field: Division of Nutritional
12 Sciences, Cornell University, 113 Savage Hall, Ithaca, NY 14853; mas246@cornell.edu; Tel.
13 (607) 255-6081

14

15

16

17

18

19

20

21

22

23

24

25

26

27

28

29

30

31

32

33

34 **ABSTRACT**

35 Background: Serine hydroxymethyltransferase 2 (SHMT2) catalyzes the reversible conversion of
36 tetrahydrofolate (THF) and serine producing THF-conjugated one-carbon units and glycine in
37 the mitochondria. Biallelic *SHMT2* variants were identified in humans and suggested to alter the
38 protein's active site, potentially disrupting enzymatic function. SHMT2 expression has also been
39 shown to decrease with aging in human fibroblasts. Immortalized cells models of total *SHMT2*
40 loss or folate deficiency exhibit decreased oxidative capacity and impaired mitochondrial
41 complex I assembly and protein levels, suggesting folate-mediated one-carbon metabolism
42 (FOCM) and the oxidative phosphorylation system are functionally coordinated. This study
43 examined the role of SHMT2 and folate availability in regulating mitochondrial function, energy
44 metabolism, and cellular proliferative capacity in both heterozygous and homozygous cell
45 models of reduced *SHMT2* expression.

46 Methods: Primary mouse embryonic fibroblasts (MEF) were isolated from a C57Bl/6 dam
47 crossed with a heterozygous *Shmt2*^{+/-} male to generate *Shmt2*^{+/+} (wild-type) or *Shmt2*^{+/-} (HET)
48 MEF cells. In addition, haploid chronic myeloid leukemia cells (HAP1, wild-type) or HAP1
49 cells lacking SHMT2 expression (Δ SHMT2) were cultured for 4 doublings in either low-folate or
50 folate-sufficient culture media. Cells were examined for proliferation, total folate levels, mtDNA
51 content, protein levels of pyruvate kinase and PGC1 α , pyruvate kinase enzyme activity,
52 mitochondrial membrane potential, and mitochondrial function.

53 Results: Homozygous loss of *SHMT2* in HAP1 cells impaired cellular folate accumulation and
54 altered mitochondrial DNA content, membrane potential, and basal respiration. Formate rescued
55 proliferation in HAP1, but not Δ SHMT2, cells cultured in low-folate medium. Pyruvate kinase
56 activity and protein levels were impaired in Δ SHMT2 cells and in MEF cells exposed to low-

57 folate medium. Mitochondrial biogenesis protein levels were elevated in *Shmt2*^{+/-} MEF cells,
58 while mitochondrial mass was increased in both homozygous and heterozygous models of
59 SHMT2 loss.

60 Conclusions: The results from this study indicate disrupted mitochondrial FOCM impairs
61 mitochondrial folate accumulation and respiration, glycolytic activity, and cellular proliferation.
62 These changes persist even after a potentially compensatory increase in mitochondrial biogenesis
63 as a result of decreased SHMT2 levels.

64 Keywords: Folate, one-carbon metabolism, SHMT2, energy metabolism, oxygen consumption
65 rate, pyruvate kinase (include 3 – 10 key words)

66
67
68
69
70
71
72
73
74
75
76
77
78
79
80
81
82
83

84 INTRODUCTION

85 Folate coenzymes, found within the folate-mediated one-carbon metabolism (FOCM)
86 metabolic network, mediate the activation and transfer of one-carbon units for diverse cellular
87 processes, including *de novo* purine and thymidylate (dTMP) biosynthesis, amino acid
88 metabolism, and methionine regeneration [1,2]. The transfer of one-carbon units is
89 compartmentalized within the nucleus, cytosol, and mitochondria [3], and serine catabolism
90 provides the majority of one-carbon units within mammalian cells [4]. Within the mitochondria,
91 serine hydroxymethyltransferase 2 (SHMT2) catalyzes the reversible conversion of
92 tetrahydrofolate (THF) and serine, producing THF-conjugated one-carbon units and glycine [5].
93 In this pathway, the majority of serine is converted to formate, which exits the mitochondria and
94 is used in the above mentioned nuclear or cytosolic FOCM processes [1,6,7]. Recently, biallelic
95 *SHMT2* variants were identified in humans and suggested to alter the protein's active site [8].
96 Indeed, patient fibroblasts from individuals with *SHMT2* variants display a decreased ratio of
97 glycine to serine, suggesting disrupted enzymatic function, though the consequences of reduced
98 activity are relatively uncharacterized.

99 Immortalized/transformed cell models of total *SHMT2* loss have been utilized to study
100 the implications of impaired mitochondrial FOCM. Many of these models have examined the
101 drivers of proliferative capacity in cancer cells, which exhibit higher levels of SHMT2 than
102 noncancer tissue [9,10]. Interestingly, changes in SHMT2 levels have also been associated with
103 aging; aged human fibroblasts exhibit reduced *SHMT2* expression corresponding with reduced
104 oxygen consumption [11], suggesting SHMT2 not only plays a role in cell proliferation but also
105 in mitochondrial energy metabolism.

106 Serine-derived one-carbon units can also be used for *de novo* dTMP biosynthesis within
107 the mitochondria [5,12]. Mitochondrial DNA (mtDNA) encodes 13 proteins that are required for
108 ATP synthesis as well as mitochondrial tRNA and rRNA molecules, and it has been recognized
109 for decades that mutations in mtDNA increase with age, lead to diseases, and occur ~100-fold
110 more frequently than in the nuclear genome [13–15]. Furthermore, reduced *Shmt2* expression
111 and folate deficiency resulted in increased uracil misincorporation in mtDNA, in a heterozygous
112 mouse model of *Shmt2* loss, without affecting uracil misincorporation in the nuclear genome
113 [16]. These findings are consistent with evidence that mtDNA is more sensitive to genomic
114 instability than nuclear DNA [17].

115 Numerous *in vitro* studies have focused on the consequences of homozygous loss of
116 *SHMT2* in immortalized/transformed cells, however, *in vivo* models of homozygous *SHMT2* loss
117 are embryonically lethal [16,18]. *SHMT2* expression also declines with age in human fibroblast
118 cells [11]. Since *SHMT2* is at the intersection of aging and cellular proliferation/mitochondrial
119 metabolism, we developed a mouse embryonic fibroblast (MEF) cell model of heterozygous
120 *Shmt2* loss to more closely mimic conditions with reduced *SHMT2*. Here, we describe the role of
121 *SHMT2* and folate availability in regulating energy metabolism and cellular proliferative
122 capacity in heterozygous and homozygous cell models of *SHMT2* expression.

123 **METHODS**

124 *Cell culture conditions*

125 HAP1 cells (wild-type) and *SHMT2* knockout HAP1 (Δ *SHMT2*) cells were obtained
126 from Horizon Discovery: Δ *SHMT2* cells were generated by Horizon Discovery using
127 CRISPR/Cas9 and contain a 2-bp deletion in *SHMT2* coding exon 2. Cells were regularly

128 passaged in Iscove's Modification of DMEM (IMDM; Corning) supplemented with 10% FBS
129 and 1% penicillin/streptomycin. Because metabolism related phenotypes often do not manifest
130 based on nutrient availability, we cultured HAP1 and Δ SHMT2 cells in 25 nM (folate-sufficient)
131 and 0 nM (folate-deficient) folate supplemented modified DMEM medium (Hyclone; formulated
132 to lack glucose, glutamine, B vitamins, methionine, glycine and serine) containing 10% fetal
133 bovine serum, 1% penicillin/streptomycin, 4.5 g/L glucose, 3 g/L sodium bicarbonate, 4 nM
134 glutamine, 200 μ M methionine, 4 mg/L pyridoxine, 30 mg/L glycine, and 25 or 0 nM (6S)-5-
135 formyl-THF.

136 Mouse embryonic fibroblasts were isolated from C57Bl/6J female mice bred to *Shmt2*^{+/-}
137 male mice as previously described [16]. All experiments include wild-type *Shmt2*^{+/+} and
138 heterozygous *Shmt2*^{+/-} MEF cells. Cells were regularly passaged in alpha-minimal essential
139 medium (alpha-MEM; Hyclone Laboratories) supplemented with 10% FBS and 1%
140 penicillin/streptomycin. For 25 and 0 nM folate supplemented experimental conditions, cells
141 were cultured in modified alpha-MEM (HyClone; lacking glycine, serine, methionine, B
142 vitamins, and nucleosides); modified alpha-MEM was supplemented with 10% dialyzed FBS,
143 200 μ M methionine, 1 mg/L pyridoxine, and 25 or 0 nM (6S)-5- formyl-THF.

144 *Cell proliferation*

145 HAP1 cells and Δ SHMT2 cells were seeded at 1000 cells per well in 96-well plates in 25
146 nM and 0 nM folate supplemented medium with the addition of 0- or 2-mM formate. The
147 number of total and dead cells was determined at specified time points by co-staining cells with
148 Hoechst 33342 (Life Technologies) and propidium iodide (Thermo Fisher Scientific),
149 respectively. Cells were visualized and quantified using a Celigo imaging cytometer (Nexcelom)
150 following the manufacturer's instructions. The number of live cells was determined by

151 subtracting the number of propidium iodide-positive cells from the Hoechst 33342-positive cells.
152 Data are shown as cell proliferation normalized to cell number on day 1.

153 *Immunoblotting*

154 Total protein was extracted following tissue lysis by sonication in lysis buffer (150 mM
155 NaCl, 5 mM EDTA pH8, 1% Triton X-100, 10 mM Tris-Cl, 5 mM dithiothreitol and protease
156 inhibitor) and quantified by the Lowry-Bensadoun assay [19]. Proteins were denatured by
157 heating with 6X Laemelli buffer for 5 min at 95 °C. Samples were electrophoresed on 8-12%
158 SDS-PAGE gels for approximately 60-70 min in SDS-PAGE running buffer and then transferred
159 to an Immobilon-P polyvinylidene difluoride membrane (Millipore Corp.) using a MiniTransblot
160 apparatus (Bio-Rad). Membranes were blocked in 5% (w/v) nonfat dairy milk in 1X TBS
161 containing 0.1% Tween-20 for 1 h at room temperature. The membranes were incubated
162 overnight in the primary antibody at 4 °C and then washed with 1X TBS containing 0.1%
163 Tween-20 and incubated with the appropriate horseradish peroxidase–conjugated secondary
164 antibody at 4 °C for 1 h at room temperature. The membranes were visualized with Clarity and
165 Clarity Max ECL Western Blotting Substrates (Bio-Rad). Antibodies against SHMT2 (Cell
166 Signaling, 1:1000), PKM1 (Cell Signaling, 1:1000), PKM2 (Cell Signaling, 1:1000), PGC1 α
167 (Cell Signaling, 1:1000), and GAPDH (Cell Signaling, 1:2000) were used. For antibody
168 detection, a goat anti-rabbit IgG-horseradish peroxidase-conjugated secondary (Pierce) was used
169 at a 1:15000 dilution. Membranes were imaged using FluorChem E (Protein Simple), and
170 densitometry was performed with ImageJ (version 1.53a) using GAPDH as the control.

171 *Folate concentration analysis*

172 Cell folate concentrations were quantified using the *Lactobacillus casei* microbiological
173 assay as previously described [20]. Total folates were normalized to protein concentrations for
174 each sample [19].

175 *Mitochondrial DNA content, membrane potential, and mitochondrial function*

176 Total genomic DNA was isolated with the Roche High Pure PCR Template Preparation
177 Kit per manufacturers' protocol. Mitochondrial DNA copy number was determined by real-time
178 quantitative PCR (Roche LightCycler® 480) as previously described [21], using LightCycler®
179 480 SYBR Green I Master (Roche) and 15 ng of DNA per reaction. Oligonucleotide primers for
180 mouse Mito (F 5'- CTAGAAACCCCGAAACCAA and R 5'-
181 CCAGCTATCACCAAGCTCGT and mouse B2M (F 5'- ATGGGAAGCCCGAACATACTG
182 and R 5'- CAGTCTCAGTGGGGGTGAAT (Integrated DNA Technologies).

183 The mitochondrial membrane potential was determined using JC-1 dye (Cayman)
184 following the manufacturer's instructions. J-aggregate (excitation/emission = 535/595 nm) and
185 monomer (excitation/emission = 484/535 nm) fluorescence was measured with a SpectraMax
186 M3 (Molecular Devices).

187 The mitochondrial function was measured using a Seahorse XFe24 Extracellular Flux
188 Analyzer (Agilent Technologies). Cells were cultured in the experimental 25 and 0 nM folate
189 conditions for 4 doublings, then seeded in the same medium and allowed to adhere for 24
190 hours. Basal respiration, ATP production, and extracellular acidification rate were determined
191 following the manufacturer's instructions for the Cell Mitochondrial Stress Test (Agilent
192 Technologies) and normalized to total cell count.

193 *Pyruvate kinase enzyme activity*

194 HAP1 cells, Δ SHMT2 cells, and MEF cells were washed with 1 X PBS, pH 7.4, and then
195 incubated with lysis buffer (50 mM Tris-HCl, pH 7.5, 1 mM EDTA, 150 mM NaCl, 1 mM DTT,
196 protease inhibitor cocktail) for 15 minutes on ice to lyse cells. Protein was quantified by a BCA
197 protein assay (Pierce) and 8 ug of fresh cell lysate was loaded per reaction following the
198 instructions of the pyruvate kinase enzyme activity assay [22]. Optical absorbance of the reaction
199 at 340 nm was measured every 15 sec for 10 min with a SpectraMax M3 (Molecular Devices).

200 *Mitochondrial mass and NAD/NADH ratio*

201 The mitochondrial mass was determined using a Citrate Synthase Activity Assay Kit
202 (Sigma-Aldrich) following the manufacturer's instructions. Number of mitochondria was
203 normalized to the total protein concentration. The NAD/NADH ratio was determined using a
204 NAD/NADH-Glo Assay (Promega) according to the manufacturer's instructions. NAD/NADH
205 ratio was normalized to total cell number determined by Hoechst 33342 (Life Technologies)
206 staining as described above.

207 *Statistical analyses*

208 JMP® Pro statistical software version 15 (SAS Institute Inc.) was used for all statistical
209 analyses. Linear mixed effects models with main effects of media, genotype, and time (with time
210 as a continuous variable), and all 2- and 3-way interactions were used to determine HAP1 and
211 Δ SHMT2 cell proliferation. For analyses in which HAP1 and Δ SHMT2 cells or *Shmt2*^{+/+} and
212 *Shmt2*^{+/-} MEF cells were cultured in 25 or 0 nM folate supplemented medium, results were
213 analyzed by two-way ANOVA with Tukey post-hoc analysis to determine genotype by medium
214 interaction and main effects of medium and genotype. For analyses in which HAP1 and
215 Δ SHMT2 cells or *Shmt2*^{+/+} and *Shmt2*^{+/-} MEF cells were compared, results were analyzed by
216 Student's *t* test. All statistics were performed at the 95% confidence level ($\alpha = 0.05$) and groups

217 were considered significantly different when $p \leq 0.05$. Descriptive statistics were calculated on
218 all variables to include means and standard deviations.

219 **RESULTS**

220 **Loss of SHMT2 impairs cellular folate accumulation and alters mitochondrial DNA** 221 **content, membrane potential, and basal respiration in HAP1 cells.**

222 We have previously demonstrated that heterozygous *Shmt2*^{+/-} MEF cells exhibited a ~50%
223 reduction in SHMT2 protein levels compared to *Shmt2*^{+/+} MEF cells, and *Shmt2*^{+/+} and *Shmt2*^{+/-}
224 MEF cells cultured in low-folate medium had a reduction in total folates [16]. To assess effects
225 of total loss of *SHMT2*, HAP1 cells and Δ SHMT2 cells were cultured in medium containing
226 either 25 nM (6S)5-formylTHF (folate-sufficient medium) or 0 nM (6S)5-formylTHF (low-folate
227 medium). The 2-bp deletion in an *SHMT2* coding exon resulted in a significant reduction in
228 SHMT2 protein levels with no visible protein in the Δ SHMT2 cells ($p < 0.01$, Figure 1A). As
229 expected, HAP1 cells and Δ SHMT2 cells grown in low-folate medium had impaired
230 accumulation of folate ($p < 0.01$, Figure 1B), and there was a significant genotype by folate
231 interaction ($p < 0.05$, Figure 1B). Δ SHMT2 cells grown in folate-sufficient medium exhibited a
232 trend toward reduced folate accumulation compared to HAP1 cells grown in folate-sufficient
233 medium ($p = 0.05$, Figure 1B), consistent with what was observed in *Shmt2*^{+/-} mouse liver [16].

234 There were significant genotype by medium interactions in mtDNA content ($p < 0.05$,
235 Figure 1C) and mitochondrial membrane potential in the HAP1 and Δ SHMT2 cells ($p < 0.001$,
236 Figure 1D). mtDNA content in HAP1 cells and Δ SHMT2 cells responded independently to folate
237 availability, with decreased mtDNA content in Δ SHMT2 cells cultured in low-folate medium
238 (Figure 1C). In addition, exposure to low-folate medium increased mitochondrial membrane

239 potential in both HAP1 and Δ SHMT2 cells ($p < 0.001$, Figure 1D). Furthermore, oxygen
240 consumption rate was impaired in Δ SHMT2 cells compared to HAP1 cells; Δ SHMT2 cells
241 cultured in folate-sufficient medium had <50% less capacity to utilize oxygen than HAP1 cells
242 cultured in folate-sufficient medium ($p < 0.01$, Figure 1E). A more modest ~20% reduction in
243 oxygen consumption was also observed in *Shmt2*^{+/-} MEF cells, and in *Shmt2*^{+/+} and *Shmt2*^{+/-}
244 MEF cells cultured in low-folate medium compared to *Shmt2*^{+/+} MEF cells [16]. Additionally,
245 *Shmt2*^{+/-} MEF cells and *Shmt2*^{+/+} and *Shmt2*^{+/-} MEF cells cultured in low-folate medium had
246 decreased mitochondrial membrane potential with no changes in mtDNA content [16].

247 **The addition of formate rescues proliferation in HAP1, but not Δ SHMT2, cells cultured**
248 **low-folate medium.**

249 We previously demonstrated that *Shmt2*^{+/-} MEF cells, and *Shmt2*^{+/+} and *Shmt2*^{+/-} MEF cells
250 cultured in low-folate medium had reduced cellular proliferation and the addition of 2 mM
251 formate restored cellular proliferation in *Shmt2*^{+/+} and *Shmt2*^{+/-} MEF cells cultured in low-folate
252 medium [16]. Examination of cell proliferation rates with total loss of *SHMT2* confirmed
253 significant effects of Δ SHMT2 genotype, exposure to low-folate media, and medium over time
254 interaction for the cell proliferation ($p < 0.001$ for all main effects and interactions; Figure 2A).
255 The genotype-driven differences in cell proliferation were significant at day 1 and became more
256 pronounced at days 2 and 3 (Figure 2B). The addition of 2 mM formate rescued growth of HAP1
257 cells cultured in low-folate medium, but not Δ SHMT2 cells in either medium type (Figure 2A
258 and 2C). This finding suggests that mitochondrial conversion of one-carbon units from serine to
259 formate is not the only growth-limiting effect of *SHMT2* loss. Interestingly, 2 mM formate
260 supplementation enhanced the proliferation capacity of HAP1 cells culture in low-folate medium
261 compared to HAP1 cells cultured in folate-sufficient medium at day 2, but the difference was lost

262 by day 3 and 4 (Figure 2C). Δ SHMT2 cells cultured in folate-sufficient IMDM medium had
263 reduced cellular proliferation compared to HAP1 cells (Figure S1A-B); furthermore, the addition
264 of formate also failed to rescue the impaired proliferation even in what is considered “complete”
265 culture medium for HAP1 cells (Figure S1A-B).

266 **Glycolytic and mitochondrial biogenesis protein levels and ATP production exhibit distinct**
267 **responses in cell models of homozygous and heterozygous *SHMT2* expression.**

268 Heterozygous disruption of *Shmt2* expression in MEF cells [16] and Δ SHMT2 cells exhibit
269 impaired oxygen consumption (Figure 1); therefore, to determine if glycolytic activity was
270 increased to compensate for the reduction in ATP generation from oxidative phosphorylation, we
271 assayed pyruvate kinase activity. Protein levels of PKM1 and PKM2 were significantly reduced
272 in Δ SHMT2 cells compared to HAP1 cells ($p < 0.01$; Figure 3A). Interestingly, protein levels of
273 PKM1 and PKM2 in *Shmt2*^{+/+} and *Shmt2*^{+/-} MEF cells were reduced only when the cells were
274 cultured in low-folate medium, with more robust changes in PKM1 protein levels compared to
275 PKM2 protein levels as a result of exposure to low-folate medium (Figure 4A). Pyruvate kinase
276 enzyme activity corresponded with the proteins levels; activity was significantly reduced in
277 Δ SHMT2 cells compared to HAP1 cells ($p < 0.001$ for genotype and genotype by medium
278 interaction; Figure 3B), and in both *Shmt2*^{+/+} and *Shmt2*^{+/-} MEF cells cultured in low-folate
279 medium ($p < 0.001$; Figure 4B). Because oxygen consumption and pyruvate kinase protein levels
280 and enzyme activity were impaired in both cell models, we evaluated ATP production and
281 extracellular acidification rates (ECAR). ATP production was significantly reduced in Δ SHMT2
282 cells compared to HAP1 cells ($p < 0.001$; Figure 5A), and in both *Shmt2*^{+/+} and *Shmt2*^{+/-} MEF
283 cells cultured in low-folate medium ($p < 0.05$; Figure 5B). Interestingly, *Shmt2*^{+/-} MEF cells
284 cultured in folate-sufficient medium exhibited a reduced ATP production compared to folate-

285 sufficient *Shmt2*^{+/+} MEF cells (Figure 5B). Furthermore, both cell models of *SHMT2* loss and
286 cells exposed to low-folate medium had reduced ECAR rates compared to the wild-type cells
287 grown in folate-sufficient medium (Figure 5A and B). To determine if mitochondrial biogenesis
288 was impacted in these models, we examined protein levels of the transcription factor PPARγ
289 Coactivator 1 Alpha (PGC1α). *Shmt2*^{+/-} MEF cells cultured in folate-sufficient medium exhibited
290 a 16-fold increase in PGC1α protein levels compared to *Shmt2*^{+/+} MEF cells (Figure 4A). PGC1α
291 protein was not detected in HAP1 cells or Δ*SHMT2* cells (data not shown).

292 **Mitochondrial mass is increased as a result of homozygous and heterozygous *SHMT2***
293 **deletion, while NAD/NADH ratio is reduced only with homozygous loss of *SHMT2*.**

294 To further evaluate markers of mitochondrial health and metabolism in the homozygous and
295 heterozygous *SHMT2* cell models, citrate synthase activity and NAD/NADH ratio were
296 measured. Citrate synthase activity (a biomarker for mitochondrial mass [23]) was significantly
297 increased in both Δ*SHMT2* cells ($p < 0.001$; Figure 6A) and *Shmt2*^{+/-} MEF cells ($p < 0.05$;
298 Figure 6B) compared to their respective wild-type cells. Additionally, there was a genotype by
299 medium interaction in HAP1 cells and Δ*SHMT2* cells cultured in low-folate and folate-sufficient
300 medium (Figure 6A). Levels of NAD/NADH in Δ*SHMT2* cells were reduced by 17% compared
301 to HAP1 cells ($p < 0.05$; Figure 7A). There were no differences in NAD/NADH comparing
302 *Shmt2*^{+/+} and *Shmt2*^{+/-} MEF cells (Figure 7B).

303 **DISCUSSION**

304 With the identification of biallelic *SHMT2* human variants [8] and the observation that
305 *SHMT2* expression in human fibroblasts is decreased with age [11], understanding the cellular
306 implications of perturbed mitochondrial FOCM is of great interest. In Δ*SHMT2* cells, we

307 observed decreased folate accumulation, which is consistent with our previous findings in
308 *Shmt2*^{+/-} liver mitochondria [16]. Since mitochondria contain approximately 40% of total cellular
309 folate [3], it is likely that the decreased whole-cell folate level in Δ SHMT2 cells is a result of
310 impaired mitochondrial folate accumulation.

311 Effects of SHMT2 loss on cellular proliferation have varied by cell type. Multiple
312 homozygous *SHMT2* deletion cell models indicate there are no changes in cellular proliferation
313 rates compared to wild-type cells [24,25]. We previously demonstrated heterozygous *Shmt2*
314 MEF cells have impaired proliferative capacity [16]. Further supporting the distinct cell type
315 response with *SHMT2* loss; Δ SHMT2 cells cultured in either a low-folate modified medium or
316 the more favorable IMDM medium (Figure 2 and S1) have impaired proliferative capacity
317 compared to HAP1 cells cultured in the same media. The cell proliferative capacity and
318 respiratory defects were not rescued by the addition of glycine in heterozygous *Shmt2* expressing
319 MEF cells [16] or in Δ SHMT2 cells, as their growth medium contained adequate glycine levels.
320 This suggests the one-carbon groups entering the folate pool from the glycine cleavage system
321 are not sufficient to overcome the loss of serine-derived one-carbon units from the mitochondria
322 to support cellular proliferation or mitochondrial function. Formate supplementation rescued
323 HAP1 cell proliferation in cells cultured in low-folate medium (Figure 2) [16]. The inability of
324 formate supplementation to rescue impaired proliferation in Δ SHMT2 cells suggests that the
325 impact of SHMT2 loss on proliferation is due to effects of SHMT2 other than simply providing
326 formate for nuclear/cytosolic FOCM, as has been suggested in other cell models [26], including
327 in MEF cells [16].

328 PKM has two isoforms, PKM1 and PKM2; PKM1 is expressed in differentiated tissues
329 (i.e., brain and muscle) while PKM2 is expressed in cancer cells, embryonic cells, and in

330 proliferating cells [27,28]. It has previously been proposed that PKM1 promotes oxidative
331 phosphorylation [26] and proliferation arrest due to a reduction in nucleotide biosynthesis [27],
332 while silencing of PKM1 impairs mitochondrial membrane potential and induces apoptosis [26].
333 In another study, PKM2 activity is upregulated when *SHMT2* expression is suppressed [24],
334 which suggests a lower level of SHMT2 would promote the conversion of phosphoenolpyruvate
335 and ADP to pyruvate and ATP. In our cell models, we found that Δ SHMT2 cells had
336 substantially reduced protein levels of PKM1 and PKM2, and reduced PK activity (Figure 3a and
337 3b). Independent of *Shmt2* expression levels, MEF cells exposed to low-folate medium had
338 severely reduced protein levels of PKM1 and PK activity, with a modest reduction in PKM2
339 protein levels (Figure 4a and 4b). To our knowledge, this is the first observation of an effect of
340 decreased cellular folate availability on PK activity. In addition, it does not appear that glycolysis
341 or lactate/hydrogen ion production is increased to compensate for the reduction in mitochondrial
342 respiration in either cell model, as both ATP production and ECAR were decreased with loss of
343 SHMT2 or folate-depletion (Figure 5a and 5b). This is also supported by other cell models of
344 SHMT2 loss that indicate the rate-limiting glycolytic proteins, hexokinase and
345 phosphofructokinase, are unchanged with loss of SHMT2 [25]; however, in this cell model
346 (293A cells), homozygous loss of SHMT2 increases lactate levels and lactate dehydrogenase
347 protein levels. In addition to the reduction in glycolytic and respiratory capacity, it has also been
348 demonstrated that the TCA cycle intermediates citrate, succinate, malate, and aspartate are lower
349 in cells with homozygous loss of SHMT2 [29]. The reduced ATP production may influence the
350 impaired proliferative capacity exhibited in Δ SHMT2 cells, *Shmt2*^{+/-} MEF cells, and MEF cells
351 exposed to low-folate medium. Of note, cell health after exposure to low-folate medium
352 indicated low cell death rates (<5%, data not shown).

353 Immortalized/transformed and MEF cell models of homozygous loss of *SHMT2* indicate
354 mitochondrial derived protein levels and respiratory capacity are severely impaired, however,
355 there were no changes in mRNA levels of these genes [18,25,30]. This supports the findings
356 from immortalized/transformed cells models of total *SHMT2* loss that suggest reduced
357 respiratory capacity results from impaired mitochondrial translation [29,31]. Interestingly, both
358 Δ *SHMT2* cells and *Shmt2*^{+/-} MEF cells have increased mitochondrial mass (Figure 6a and 6b),
359 suggesting increased mitochondrial number in an attempt to compensate for reduced
360 mitochondrial function. The inability to correct the impaired mitochondrial function could be
361 from uracil misincorporation in mtDNA, as exhibited in *Shmt2*^{+/-} mice or *Shmt2*^{+/+} mice
362 exposed to low-folate diet for 7 weeks [16], potentially causing genomic instability. The
363 mitochondrial mass in both cell types was increased in response to loss of SHMT2, however the
364 overall mitochondrial mass in HAP1 derived cells was much lower than in MEF cells. Another
365 compensatory response that was only seen in *Shmt2*^{+/-} MEF cells was increased PGC1 α protein
366 levels. The robust increase in PGC1 α protein levels in *Shmt2*^{+/-} MEF cells is consistent with
367 increased mitochondrial biogenesis (i.e., increased mitochondrial mass, Figure 6b).

368 Regardless of whether loss of SHMT2 or folate-depletion influence mitochondrial protein
369 translation or nucleotide biosynthesis, these findings support the notion that SHMT2 and
370 adequate folate are essential for mitochondrial function. This may have important implications
371 for older adults, as *SHMT2* expression in human fibroblasts declines with age [11]. Furthermore,
372 because our cell models and that of others yield different responses, this indicates there may be
373 tissue-specific responses to loss of SHMT2. Taken together, understanding age-associated
374 changes in *SHMT2* expression levels, and investigating tissue-specific changes in response to
375 reduced *SHMT2* should be assessed in future work.

376 CONCLUSIONS

377 In this study, heterozygous and homozygous cell models of *SHMT2* expression exposed
378 to low or adequate levels of folate were investigated. The results demonstrate that disrupted
379 mitochondrial FOCM impairs mitochondrial folate accumulation and respiration, pyruvate kinase
380 activity, and cellular proliferation. These findings provide evidence for the essentiality of
381 *SHMT2* and folate in maintaining energy production and have important implications for
382 individuals with *SHMT2* variants and in aging individuals.

383 Abbreviations: dTMP, thymidine monophosphate; FD, folate-deficient; FOCM, folate-mediated
384 one-carbon metabolism; GAPDH, glyceraldehyde-3 phosphate dehydrogenase; IMDM, Iscove's
385 modification of DMEM; MEF, murine embryonic fibroblast; MEM, minimal essential medium;
386 mtDNA, mitochondrial DNA; PKM1, pyruvate kinase M1; OCR, oxygen consumption rate;
387 PKM2, pyruvate kinase M2; PGC1 α , PPAR γ coactivator-1 α ; *SHMT2*, serine
388 hydroxymethyltransferase 2; THF, tetrahydrofolate.

389 Declarations

390 Animal ethics approval: All mice were maintained under specific pathogen-free conditions in
391 accordance with standard of use protocols and animal welfare regulations. All study protocols
392 were approved by the Institutional Animal Care and Use Committee of Cornell University.

393 Consent for publication: NA

394 Availability of data and materials: All data generated or analyzed during this study are included
395 in this published article [and its supplementary information files].

396 Competing interests: The authors declare that they have no conflicts of interest with the contents
397 of this article.

398 Funding: This study was financially supported by a President's Council of Cornell Women
399 Award. Supported by National Science Foundation Graduate Research Fellowship Program grant
400 DGE-1650441 (to JEB).

401 Authors' contributions: JLF and MSF designed research; JLF, LFC, and JEB conducted research;
402 JLF and MSF analyzed data; JLF and MSF prepared the manuscript; and MSF has primary
403 responsibility for the final content. All authors read and approved the final manuscript.

404 Acknowledgements: NA

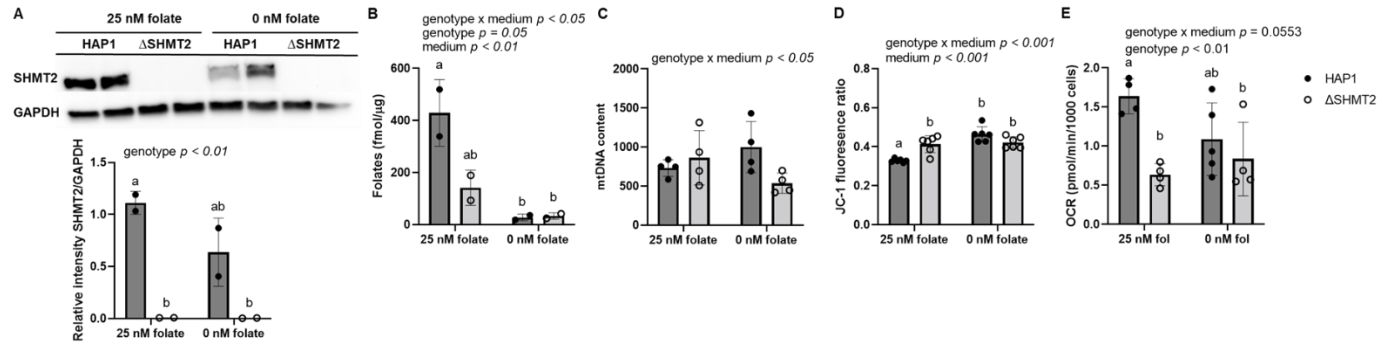
References

1. Tibbetts AS, Appling DR. Compartmentalization of mammalian folate-mediated one-carbon metabolism. *Annu. Rev. Nutr.* 2010. p. 57–81.
2. Xiu Y, Field MS. The roles of mitochondrial folate metabolism in supporting mitochondrial DNA synthesis, oxidative phosphorylation, and cellular function. *Curr. Dev. Nutr.* Oxford University Press; 2020.
3. Lan X, Field MS, Stover PJ. Cell cycle regulation of folate-mediated one-carbon metabolism. *Wiley Interdiscip. Rev. Syst. Biol. Med.* 2018. p. e1426.
4. De Koning TJ, Snell K, Duran M, Berger R, Poll-The BT, Surtees R. L-serine in disease and development. *Biochem. J.* 2003. p. 653–61.
5. Anderson DD, Quintero CM, Stover PJ. Identification of a de novo thymidylate biosynthesis pathway in mammalian mitochondria. *Proc Natl Acad Sci U S A.* 2011;108:15163–8.
6. Spizzichino S, Boi D, Boumis G, Lucchi R, Liberati FR, Capelli D, et al. Cytosolic localization and in vitro assembly of human de novo thymidylate synthesis complex. *FEBS J.* 2021.
7. Xiu Y, Field MS. The Roles of Mitochondrial Folate Metabolism in Supporting Mitochondrial DNA Synthesis, Oxidative Phosphorylation, and Cellular Function. *Curr Dev Nutr.* 2020;4:nzaa153.
8. García-Cazorla À, Verdura E, Juliá-Palacios N, Anderson EN, Goicoechea L, Planas-Serra L, et al. Impairment of the mitochondrial one-carbon metabolism enzyme SHMT2 causes a novel brain and heart developmental syndrome. *Acta Neuropathol.* 2020;140:971–5.

9. Yang X, Wang Z, Li X, Liu B, Liu M, Liu L, et al. Shmt2 desuccinylation by SIRT5 drives cancer cell proliferation. *Cancer Res.* 2018;78:372–86.
10. Lee GY, Haverty PM, Li L, Kljavin NM, Bourgon R, Lee J, et al. Comparative oncogenomics identifies psmb4 and shmt2 as potential cancer driver genes. *Cancer Res.* 2014;74:3114–26.
11. Hashizume O, Ohnishi S, Mito T, Shimizu A, Iashikawa K, Nakada K, et al. Epigenetic regulation of the nuclear-coded GCAT and SHMT2 genes confers human age-associated mitochondrial respiration defects. *Sci Rep.* 2015;5:1–11.
12. Anderson DD, Woeller CF, Chiang EP, Shane B, Stover PJ. Serine hydroxymethyltransferase anchors de Novo thymidylate synthesis pathway to nuclear lamina for DNA synthesis. *J Biol Chem.* 2012;287:7051–62.
13. Crott JW, Choi SW, Branda RF, Mason JB. Accumulation of mitochondrial DNA deletions is age, tissue and folate-dependent in rats. *Mutat Res - Fundam Mol Mech Mutagen.* 2005;570:63–70.
14. Chial, H. & Craig J. mtDNA and Mitochondrial Diseases. *Nat Educ.* 2008;1:217.
15. Bratic A, Larsson NG. The role of mitochondria in aging. *J Clin Invest.* 2013;123:951–7.
16. Fiddler JL, Xiu Y, Blum JE, Lamarre SG, Phinney WN, Stabler SP, et al. Reduced Shmt2 expression impairs mitochondrial folate accumulation and respiration, and leads to uracil accumulation in mouse mitochondrial DNA. *J Nutr.* 2021;151:2882–93.
17. Nadalutti CA, Ayala-Peña S, Santos JH. Mitochondrial DNA damage as driver of cellular outcomes. *Am J Physiol - Cell Physiol.* 2022;322:C136–50.

18. Tani H, Ohnishi S, Shitara H, Mito T, Yamaguchi M, Yonekawa H, et al. Mice deficient in the Shmt2 gene have mitochondrial respiration defects and are embryonic lethal. *Sci Rep*. 2018;8:1–8.
19. Bensadoun A, Weinstein D. Assay of proteins in the presence of interfering materials. *Anal Biochem*. 1976;70:241–50.
20. Horne DW, Patterson D. Lactobacillus casei microbiological assay of folic acid derivatives in 96-well microtiter plates. *Clin Chem*. 1988;34:2357–9.
21. Malik AN, Czajka A, Cunningham P. Accurate quantification of mouse mitochondrial DNA without co-amplification of nuclear mitochondrial insertion sequences. *Mitochondrion*. 2016;29:59–64.
22. Teslaa T, Teitell MA. Techniques to monitor glycolysis. *Methods Enzymol*. 2014. p. 91–114.
23. Vigelsø A, Andersen NB, Dela F. The relationship between skeletal muscle mitochondrial citrate synthase activity and whole body oxygen uptake adaptations in response to exercise training. *Int J Physiol Pathophysiol Pharmacol*. 2014;6:84.
24. Kim D, Fiske BP, Birsoy K, Freinkman E, Kami K, Possemato R, et al. SHMT2 drives glioma cell survival in the tumor microenvironment but imposes a dependence on glycine clearance. *Nature*. 2015;520:363–7.
25. Lucas S, Chen G, Aras S, Wang J. Serine catabolism is essential to maintain mitochondrial respiration in mammalian cells. *Life Sci Alliance*. 2018;1:e201800036.
26. Meiser J, Tumanov S, Maddocks O, Labuschagne CF, Athineos D, Van Den Broek N, et al. Serine one-carbon catabolism with formate overflow. *Sci Adv*. 2016;2.

27. Taniguchi K, Sakai M, Sugito N, Kuranaga Y, Kumazaki M, Shinohara H, et al. PKM1 is involved in resistance to anti-cancer drugs. *Biochem Biophys Res Commun*. 2016;473.
28. Lunt SY, Muralidhar V, Hosios AM, Israelsen WJ, Gui DY, Newhouse L, et al. Pyruvate kinase isoform expression alters nucleotide synthesis to impact cell proliferation. *Mol Cell*. 2015;57.
29. Morscher RJ, Ducker GS, Li SHJ, Mayer JA, Gitai Z, Sperl W, et al. Mitochondrial translation requires folate-dependent tRNA methylation. *Nature*. 2018;554:128–32.
30. Balsa E, Perry EA, Bennett CF, Jedrychowski M, Gygi SP, Doench JG, et al. Defective NADPH production in mitochondrial disease complex I causes inflammation and cell death. *Nat Commun*. 2020;11:1–12.
31. Minton DR, Nam M, McLaughlin DJ, Shin J, Bayraktar EC, Alvarez SW, et al. Serine Catabolism by SHMT2 Is Required for Proper Mitochondrial Translation Initiation and Maintenance of Formylmethionyl-tRNAs. *Mol Cell*. 2018;69:610–21.



405

406 **Figure 1 Homozygous loss of *SHMT2* and low-folate medium decrease folate accumulation**

407 **and basal respiration and increase mitochondrial membrane potential in HAP1 cells.**

408 A) *SHMT2* protein levels, B) total folate levels, C) mtDNA content, D) mitochondrial membrane

409 potential, and E) oxygen consumption rate in HAP1 cells and Δ *SHMT2* cells. *SHMT2* protein

410 levels were normalized to GAPDH, and densitometry was performed using ImageJ. Two-way

411 ANOVA with Tukey's post-hoc analysis was used to determine media by genotype interaction

412 and main effects of media and genotype with a statistical significance at $p < 0.05$. Levels not

413 connected by the same letter are significantly different. Data represent means \pm SD values, $n = 2-$

414 6 per group. GAPDH, glyceraldehyde-3 phosphate dehydrogenase; *SHMT2*, serine

415 hydroxymethyltransferase 2.

416

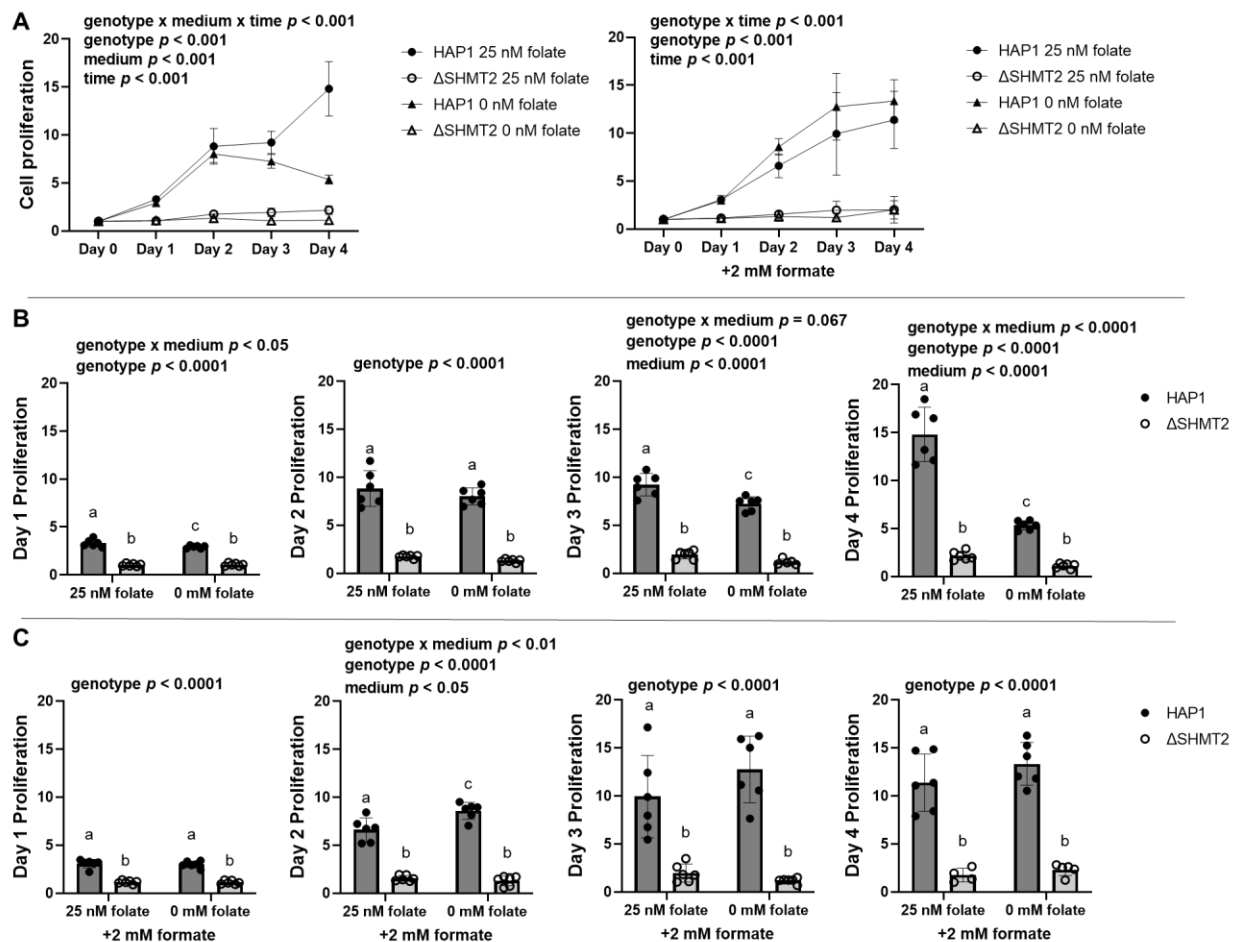
417

418

419

420

421



422

423 **Figure 2 Formate rescues cell proliferation rate in HAP1 cells cultured in low-folate**
424 **medium but not in Δ SHMT2 cells.**

425 Cell proliferation rates of Δ SHMT2 cells were compared with HAP1 cells by co-staining cells
426 with Hoechst 33342 (to identify all cells) and propidium iodide (to identify dead cells). Fold
427 change of each group was calculated by dividing by day 0 cell number. Data represent means \pm
428 SD values. Values represent n=6 replicates of cell lines cultured in medium containing either 25
429 nM (6S)5-formyl-THF or 0 nM (6S)5-formyl-THF. A) Cell proliferation rate and cell
430 proliferation rate in the presence of 2 mM formate, B) relative day 1-4 quantitation of cell
431 proliferation rate, and C) relative day 1-4 quantitation cell proliferation rate in the presence of 2

432 mM formate. Linear mixed effects models with main effects of media, genotype, and time (with
433 time as a continuous variable), and 2- and 3-way interactions were used to determine cell
434 proliferation with a statistical significance at $p < 0.05$. Two-way ANOVA with Tukey's post-hoc
435 analysis was used to determine media by genotype interaction and main effects of media and
436 genotype with a statistical significance at $p < 0.05$ were used to analyze individual day
437 proliferation. Levels not connected by the same letter are significantly different.

438

439

440

441

442

443

444

445

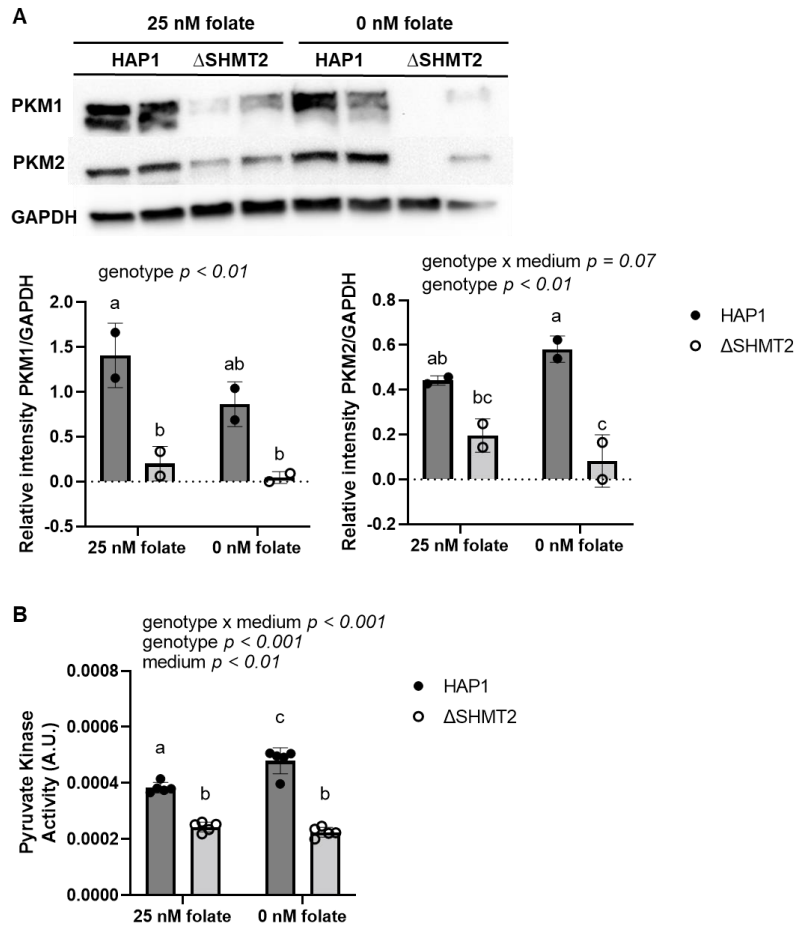
446

447

448

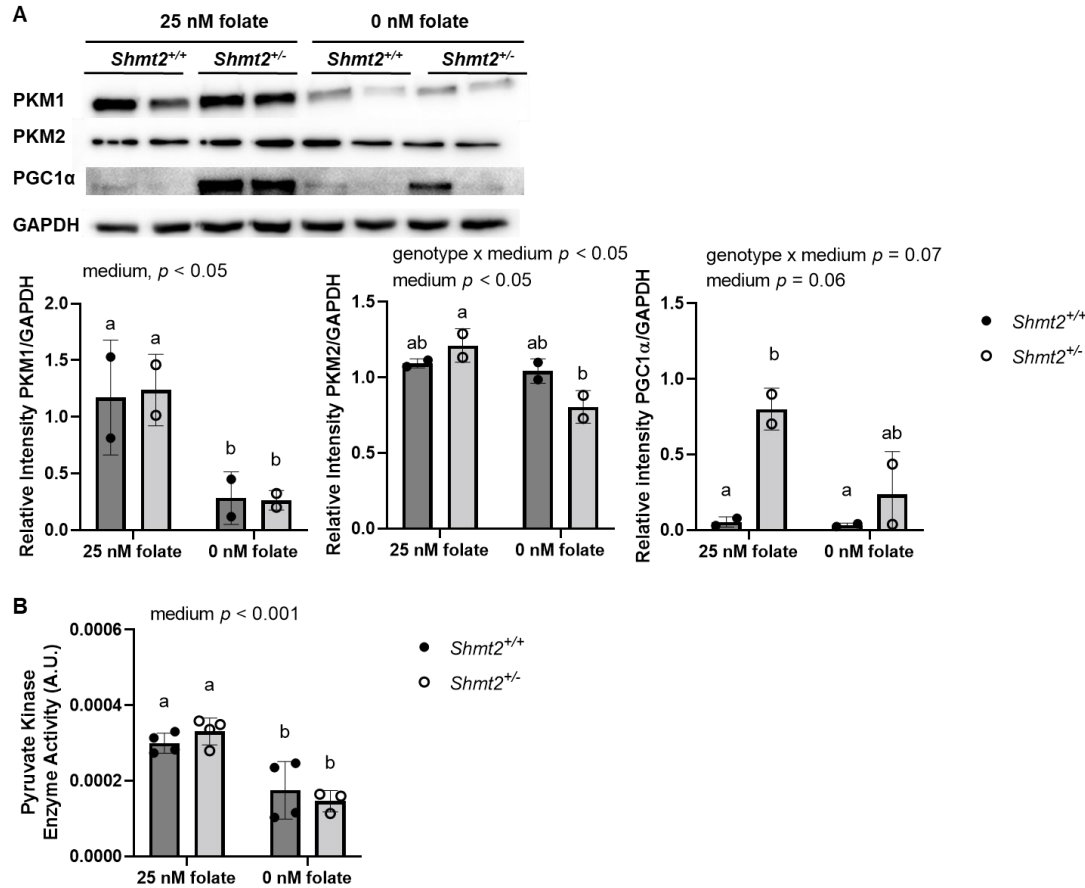
449

450



452 **Figure 3 Homozygous loss of *SHMT2* reduces protein levels and activity of pyruvate kinase**
 453 **in HAP1 cells.**

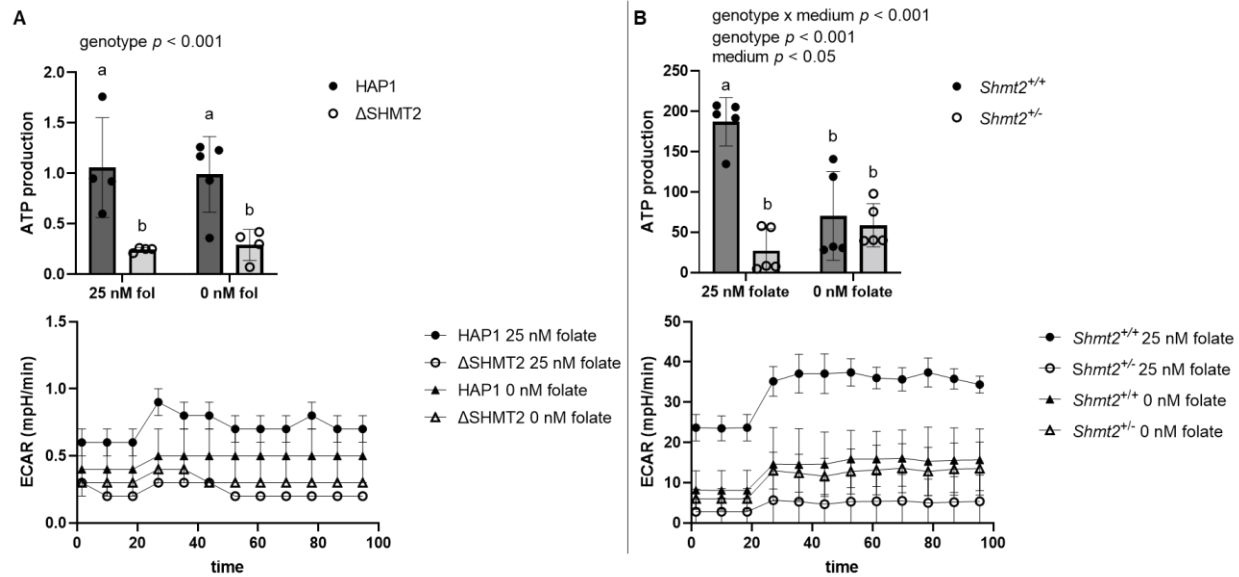
454 A) PKM1 and PKM2 protein levels and B) pyruvate kinase activity in HAP1 cells and Δ SHMT2
 455 cells. PKM1 and PKM2 protein levels were normalized to GAPDH and densitometry was
 456 performed using ImageJ. Two-way ANOVA with Tukey's post-hoc analysis was used to
 457 determine media by genotype interaction and main effects of media and genotype with a
 458 statistical significance at $p < 0.05$. Levels not connected by the same letter are significantly
 459 different. Data represent means \pm SD values, $n = 2-5$ per group. GAPDH, glyceraldehyde-3
 460 phosphate dehydrogenase; PKM1 and PKM2, pyruvate kinase M1 and M2 isoforms.



461

462 **Figure 4 Low-folate medium decreases protein levels and activity of pyruvate kinase in**
 463 **MEF cells and reduced *Shmt2* expression increases PGC1α protein levels.**

464 A) PKM1, PKM2, and PGC1α protein levels and B) pyruvate kinase activity in *Shmt2*^{+/+} and
 465 *Shmt2*^{+/-} MEF cells. PKM1, PKM2, and PGC1α protein levels were normalized to GAPDH and
 466 densitometry was performed using ImageJ. Two-way ANOVA with Tukey's post-hoc analysis
 467 was used to determine media by genotype interaction and main effects of media and genotype
 468 with a statistical significance at $p < 0.05$. Levels not connected by the same letter are
 469 significantly different. Data represent means \pm SD values, $n = 2-4$ per group with 2 embryo cells
 470 lines represented in each group. GAPDH, glyceraldehyde-3 phosphate dehydrogenase; PGC1α,
 471 PPARγ coactivator-1α; PKM1 and PKM2, pyruvate kinase M1 and M2 isoforms.



472

473 **Figure 5 Decreased SHMT2 and exposure to low-folate medium impair ATP production**
474 **and ECAR.**

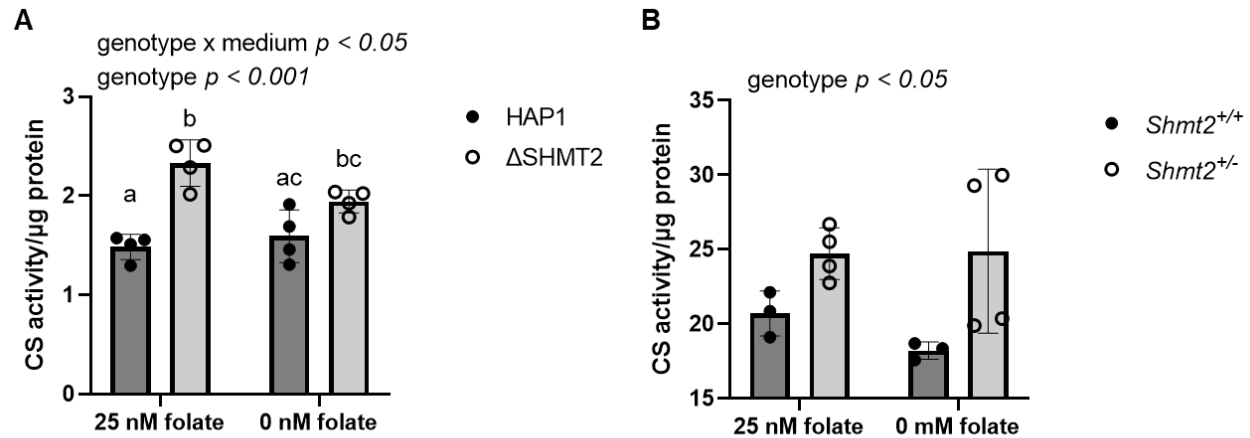
475 ATP production and extracellular acidification rates in A) HAP1 cells and Δ SHMT2 cells and B)
476 $Shmt2^{+/+}$ and $Shmt2^{+/-}$ MEF cells. ATP production and extracellular acidification rates were
477 normalized to total cell count. Two-way ANOVA with Tukey's post-hoc analysis was used to
478 determine media by genotype interaction and main effects of media and genotype with a
479 statistical significance at $p < 0.05$. Levels not connected by the same letter are significantly
480 different. Data represent means \pm SD values, n = 4 per group with 2 embryo cells lines
481 represented in each group.

482

483

484

485



486

487 **Figure 6 Decreased SHMT2 leads to increased mitochondrial mass.**

488 Citrate synthase activity in A) HAP1 cells and Δ SHMT2 cells and B) $Shmt2^{+/+}$ and $Shmt2^{+/-}$

489 MEF cells. Citrate synthase activity was normalized to total protein. Two-way ANOVA with

490 Tukey's post-hoc analysis was used to determine media by genotype interaction and main effects

491 of media and genotype with a statistical significance at $p < 0.05$. Levels not connected by the

492 same letter are significantly different. Data represent means \pm SD values, $n = 4$ per group with 2

493 embryo cells lines represented in each group. CS, citrate synthase.

494

495

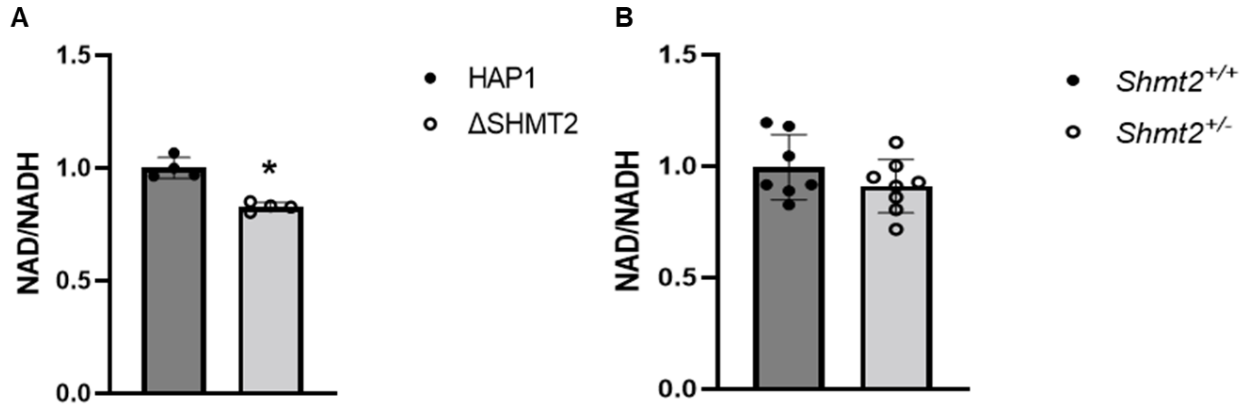
496

497

498

499

500



501

502 **Figure 7 NAD/NADH ratio is impaired with homozygous *SHMT2* loss but not heterozygous**
503 **loss.**

504 NAD/NADH ratio in A) HAP1 cells and Δ SHMT2 cells and B) $Shmt2^{+/+}$ and $Shmt2^{+/-}$ MEF
505 cells. NAD/NADH ratio was normalized to total cell count. Two-way ANOVA with Tukey's
506 post-hoc analysis was used to determine media by genotype interaction and main effects of
507 media and genotype with a statistical significance at $p < 0.05$. Levels not connected by the same
508 letter are significantly different. Data represent means \pm SD values, n = 4 per group with 2
509 embryo cells lines represented in each group.